



## On the mechanics of fishscale structures

Franck J. Vernerey<sup>a,\*</sup>, Francois Barthelat<sup>b</sup>

<sup>a</sup> Department of Civil, Environmental and Architectural Engineering, University of Colorado, Boulder, USA

<sup>b</sup> Department of Mechanical Engineering, McGill University, Montreal, Canada

### ARTICLE INFO

#### Article history:

Received 21 January 2010

Received in revised form 13 April 2010

Available online 28 April 2010

#### Keywords:

Biological structures

Flexible composite

Biomimetics

### ABSTRACT

Biological and manmade structures often share the same specifications and design constraints: structural support, lightweight or protection against specific threats. In this context, the structure of fishscales, consisting of small rigid plates growing out of the skin of a majority of fish species, are characterized by a large variety of shape, size and properties in order to achieve particular functions. The present study introduces a basic two-dimensional micromechanical model that permits to establish a correlation between the flexural response of a scaled skin and the nature of its underlying structure, including both geometric and material aspects. The model is used to predict trends in the structure's response and illustrates the fact that the scale design, arrangement and properties can be tailored to achieve a wide spectrum of response. In particular, fishscale structure possesses an inherent strain-stiffening response that can be suppressed or magnified by certain structural features. This particularity, shared by most biological materials, ensures that the structure provides both a structural and protective support for the animal.

© 2010 Elsevier Ltd. All rights reserved.

### 1. Introduction

Natural and manmade materials often share the same specifications and design constraints: structural support, lightweight or protection against certain threats. However, in most cases, nature takes a different route to solving the same engineering problems (Vincent et al., 2006), and does so by adopting highly efficient solutions (Gibson et al., 1995). Nature can therefore serve as a significant source of inspiration for new and alternative engineering designs (Barthelat, 2007). Following these concepts, biomimetics (the science of imitating nature) has recently started to yield materials with remarkable properties (Sanchez et al., 2005). The natural materials that served as models for these recent developments include seashells (Barthelat et al., 2007) or toucan beaks (Meyers et al., 2006). The mechanical performance of these natural materials comes from a complex ordered microstructure, organized over several length scales (hierarchical structure) and made of relatively weak constituents. A fundamental understanding of the relationship between structure and function is therefore required and will give invaluable insight in how to design tomorrow's engineering materials (Vincent et al., 2006). A wide array of advanced experiments and mechanistic models (Ballarini et al., 2005; Barthelat et al., 2007) are therefore being deployed in order to better understand these remarkable materials. In parallel, artificial materials inspired by nature have already started to emerge (Chen et al., 2007; Tang et al., 2003).

This paper deals with the structure and mechanics of scaled skin. Scales provide a flexible and protective outer layer on the dermis of a large variety of fish and reptilians. Fish skin (dermis and scale) has remarkable mechanical properties: lightweight, compliance, resistance to penetration, all of these in the context of an ultra-thin structure. Surprisingly this material has received little attention from the materials development community and very few experimental measurements are available. In fact, there is wide variety of different type of fishscale structures in nature, making the study of such materials a challenging task. For instance, in terms of size and arrangement, scales exhibit a great variability in shape (general classification include Cosmoid, Ganoid, Placoid and Leptoid (Kardong, 2008)), size ( $\text{mm} < \ell < \text{dm}$ ) and arrangement. In terms of properties, Ikoma et al. (2003) characterized the structure of elasmoid scales from sea bream (*Pagrus major*), a type of scale composed of mineralized collagen fibers. Tensile test on individual scales showed nonlinearity and a progressive failure, with a relatively high modulus (2.2 GPa) and tensile strength (90 MPa). In terms of biological function, Bruet et al. showed how the bony scales from an ancient family of fishes perform very well in resisting penetration and dissipating energy (Bruet et al., 2008). While the full range of fishscale function is not currently known, preliminary observations showed that it performs extremely well in a variety of tasks. In addition to having excellent hydrodynamics properties (Sudo et al., 2002), fishscales provide a protective layer resisting penetration and providing a physical barrier against attack from predators. At larger lengths, the arrangement of the scales provides a flexible skin that allows for changes in shape. In fact, the scaled skin has been showed to play a critical structural role in fish locomotion

\* Corresponding author.

E-mail address: [franck.vernerey@colorado.edu](mailto:franck.vernerey@colorado.edu) (F.J. Vernerey).

by regulating wave propagation (Long et al., 2002, 1996, 2006) and by acting as an external tendon (Hebrank and Hebrank, 1986, 1982), storing mechanical energy in order to make swimming more efficient. The structure of scaled skin at the macro level has probably inspired the scaled armor used by ancient Roman military to provide resistance to penetration while retaining relative freedom of movement. More recently, scaled skin probably also inspired more modern armor systems. While these personal armors share some mechanisms with natural fishscale, no systematic biomimetic “transfer of technology” was attempted so far, partly because a fundamental understanding of the mechanics of fish skin is still lacking.

While the above studies improve our understanding on the scaled skin properties of specific fish species and on the potential functions of fish-skins, they do not present a general picture of the underlying mechanics of fishscale structure, clearly showing how the scale microstructure influences the properties and function of the skin. Further, while the hierarchical organization of the fish skin probably plays a crucial role in its overall mechanical performance (Fratzl and Weinkamer, 2007), the contribution and synergies of each length scale has yet to be investigated. For example, how neighboring scales interact to prevent penetration and minimize skin deflection is not known. Such understanding is critical to the duplication of the performance of natural fishscales into next generation ultra-light compliant armor systems. To address these issues, this paper proposes to develop a mathematical model to quantify the mechanical behavior of a very common scales structure that can be observed on a variety of fish (known as cosmoid scales) and reptilians. In particular, due to its simplicity, the proposed theoretical/computational approach has the ability to sweep a very wide spectrum of possible fishscale structures (described by scale geometry, arrangement and properties) and correlate such structures to the overall properties of a skin. The contributions of this work are threefold: (i) understand the general behavior of fishscale structures in terms of their underlying microstructure, (ii) provide a benchmark problem that can be used as a reference for more complicated models of fishscales and (iii) provide a theoretical basis that can guide experimental tests of fish-skin.

To achieve these goals, the present study uses homogenization principles to relate structural deformation of individual scales and macroscopic response of the entire skin (Vernerey et al., 2007a,b, 2009). More specifically, we introduce a two-dimensional model that bridges deformation mechanisms occurring at the level of single scales to the overall flexural response fish-skin. The model is based on a simplified description of a fishscale structure as a two-dimensional periodic arrangement of interacting scales, attached to a circular arc, whose radius defines the macroscopic curvature of the structure. In this model, scale equilibrium is determined by considering contact interactions between adjacent scales and support reaction between scale and support and scale deformation is determined from a finite deformation beam theory. A finite element formulation is then used to study the relation between single scale deformation and macroscopic response in terms of relevant structural parameters, including scale density, scale bending and shear stiffness as well as friction. The present study shows that the mechanical response of the scaled skin is highly sensitive to the nature of its underlying structure. In addition, the structure possesses inherent strain-stiffening mechanisms that are shared by many other types of biological structures.

The paper is organized as follows. In the next section, we describe the micromechanical model for fishscale structures as well as its numerical implementation. Section 3 then concentrates on the homogenization procedure and the investigation of the mechanics of the structure when various types of microstructures are considered. Finally, Sections 4 and 5 provide a discussion and concluding remarks.

## 2. The model

In its biological context, the study of the mechanical behavior of fishscales and their interactions with the surrounding organs and muscles and skeletal structure leads to a very complex problem. To reduce this complexity, it is thus of interest to concentrate on individual components of the structure, without considering their interactions with other parts. This paper proposes to concentrate on the deformation of a population of elastic scales on the surface of dermis of fish and understand how they affect the overall mechanical behavior of the skin. This study also seeks to quantify the changes in overall skin properties (in bending) due to modifications in scale shape, arrangement and properties.

Following fundamental engineering principles, we investigate this problem by introducing an idealized model of fishscale structures, which, despite its simplicity, contains the principal ingredients of fishscale deformation during bending. Our idealized model of fishscale structure is can thus be described as follows. In its initial configuration, the scale-structure is represented as a two-dimensional arrangement of initially straight scales, lying on a straight support. Scale deformation is then restricted by its attachment to the support (on its left end) and a rotational spring resisting scale rotation at its attachment point. Assuming that the support’s rigidity is large in comparison to that of individual scales, its deformation is described in terms of homogeneous curvature  $\kappa$ . In other words, during bending, the support shape is described as an arc circle of radius  $R = 1/\kappa$  (Fig. 1), which results in the rotation and deformation of scales and the development of contact forces between adjacent scales. The elastic energy stored in this deformed configuration determines the bending stiffness of the fish-structure. To further simplify the system, one may take advantage of two distinct features of fishscale structures: (i) the fishscale structure is made of a periodic pattern and (ii) during uniform bending deformation, every scale undergoes the same deformation. These hypotheses allow us to greatly reduce the size of the problem by considering the mechanics of a single representative fishscale instead of a large assembly of them. Microstructural characteristics such as scale size, arrangement, and properties can thus be entirely described in terms of this single scale geometry and applied boundary conditions (Fig. 1). This simple model can then be used obtain a relationship between the macroscopic response of a scaled skin and the nature of its underlying structure. The free-body diagram of a fishscale subjected to several applied forces and moments arising from dermis-scale and scale-scale interactions is depicted in Fig. 1. In particular, we consider:

- The force exerted by the left scale applied at the point of contact. This force is comprised of a normal force  $\mathbf{f}_n^L$  and a tangential force  $\mathbf{f}_t^L$  resulting from friction.
- The force exerted by the right scale applied at the right extremity of the principal scale. This force can also be decomposed into a normal  $\mathbf{f}_n^R$  and tangential  $\mathbf{f}_t^R$  component, with respect to the right scale. Because of the periodicity argument, the magnitude of these forces is equal and opposite to  $\mathbf{f}_n^L$  and  $\mathbf{f}_t^L$ .
- A moment  $m^D$  resisting scale rotation around its support.

**Remark 1.** In the proposed model, assumption of a constant curvature of the support allows us to neglect the effect of local support deformation and concentrate on the response from fishscales exclusively. Interaction between fishscales and a flexible support may be considered and a more realistic model, left for future studies. This will be a particular interest to study the interaction between fishscales and soft tissue deformation, which can be an important aspect of fish-skin deformation in certain conditions (Brainerd, 1994a,b).

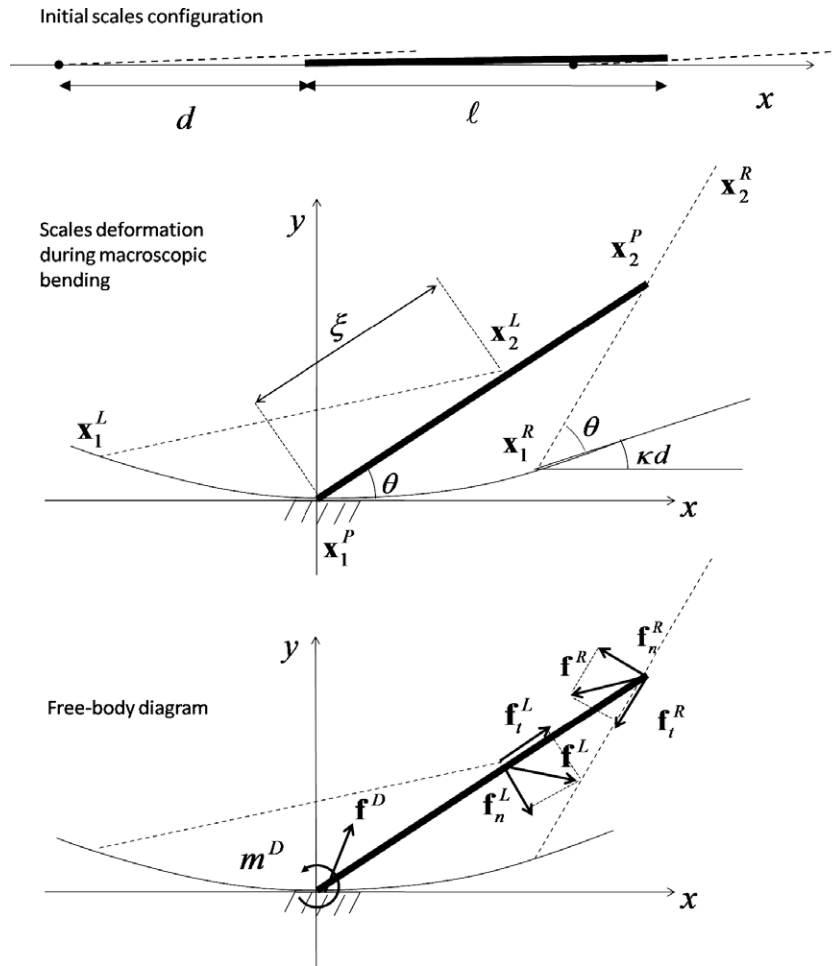


**Fig. 1.** Initial, deformed configuration and free body diagram of a primary (representative) scale (bold line) during macroscopic bending. Adjacent (left and right) scales are also shown by dotted lines for clarity.

**Remark 2.** The above model implicitly assumes that the contact between scales can be considered a point-wise interactions. While this situation may differ slightly from a real distributed scale-scale contact, this assumption will provide a first good approximation of the interaction.

With these assumptions, the method consists of computing the equilibrium configuration of the Representative scale for different values of the overall (macroscale) curvature  $\kappa$ . Referring to Fig. 1, as  $\kappa$  is varied, the position of the right scale (and thus the force  $\mathbf{f}^R$ ) changes. This results in a redistribution of forces and moment in the scale and at the contact points. The elastic energy stored in the system can then be computed and used to determine the macroscopic elastic energy, that in turn is used to compute the macroscopic moment. This procedure therefore allows the determination of the macroscopic moment–curvature response. We next describe the mathematical formulation of the problem, emphasizing on two aspects: the mechanics and deformation of the representative scale and the computation of contact forces.

### 2.1. Deformation of a single scale

In our two-dimensional analysis, the cross-section of a scale is viewed as a beam undergoing a combination of shear, axial and bending deformations. During macroscale bending, each scale may undergo a significant amount of deformation depending on their geometry and properties. It is thus essential to incorporate the nonlinear effect of finite rotation and deformation into our

model. The approach taken in this analysis relies on a hybrid analytical-computational formulation for which details can be found in (Vernerey, in preparation). In a nutshell, the method consists in solving a nonlinear ordinary differential equation for the orientation  $\phi$  of the beam's centroid, that takes the form:

$$U = EI \frac{\partial^2}{\partial s^2} (\phi - \phi_0) + g(s) = 0 \quad (1)$$

where  $E$  and  $I$  are the Young's modulus and moment of inertia of the scale's cross-section,  $\phi_0$  is the initial orientation of the beam's centroid and  $s$  is the curvilinear coordinate, referring to the initial scale configuration. The function  $g$  is a nonlinear function of the beam's orientation and the applied forces whose general expression is given by:

$$g(s) = \mathbf{w} \diamond \mathbf{F} + \alpha \mathbf{F} \cdot \mathbf{P}_1 \cdot \mathbf{F} - m \quad (2)$$

where the operation  $\diamond$  is defined as  $\mathbf{w} \diamond \mathbf{F} = w_x F_y - w_y F_x$  and the vector  $\mathbf{w}$  and matrix  $\mathbf{P}_1$  are functions of the beam's orientation as shown in Appendix A. In addition,  $\mathbf{F}$  is an integral measure of the forces  $\mathbf{f}^L$ ,  $\mathbf{f}^R$  applied on the beam (see Appendix A for details) and  $m$  is the applied moment at point  $s$ . In our particular case, we have:

$$m(0) = m^D \quad \text{and} \quad m = 0 \quad \text{when} \quad x \neq 0 \quad (3)$$

Finally, the constant  $\alpha$  is written in term of the shear modulus  $G$ , axial modulus  $E$  and the beam cross-section  $A$  as follows:

$$\alpha = \frac{1}{2} \left( \frac{1}{EA} - \frac{1}{GA} \right) \quad (4)$$

Upon solving for the beam's orientation  $\phi = \phi(s)$ , the deformed shape of the scale, given by the coordinate  $\mathbf{x} = (x(s), y(s))$  of points on the centroid, is calculated as follows:

$$\mathbf{x}(s) = \mathbf{x}(0) + \int_0^s \mathbf{q}(\phi(\xi)) d\xi \quad (5)$$

where the expression for  $\mathbf{q}$  is an explicit function of  $\phi$  and applied forces that takes the form:

$$\mathbf{q}(\phi) = \mathbf{w} + \mathbf{P}_2 \cdot \mathbf{F} \quad (6)$$

where the form of the matrix  $\mathbf{P}_2$  is given in Appendix A. The above formulation is a very efficient way to investigate the large deformation of a beam, including bending, shear, axial deformation and buckling (Vernerey, in preparation).

## 2.2. Scale-scale and dermis-scale interactions

In addition to scale deformation, the model should characterize the magnitude, direction and point of application of scale-scale forces as well as the moment  $m^D$  representing the attachment between scale and dermis. For this, let us define  $f$  as the magnitude of the normal contact force between two scales,  $\xi$  as the coordinate of the contact point, measured from the attachment in the curvilinear coordinate system and  $\kappa$  as the macroscale curvature. Denoting  $\mathbf{n}_\xi$  as the unit vector normal to the scale centroid at contact point  $\xi$ , the normal contact force  $\mathbf{f}_n^l$  is written:

$$\mathbf{f}_n^l = -f \mathbf{n}_\xi \quad (7)$$

In order to compute the contact force  $\mathbf{f}_n^R$ , we first need to realize that the orientation difference between two adjacent scales is given by the product  $\kappa d$ , where  $d$  is the inter-scale distance (Fig. 1). Thus, it is straightforward to show that:

$$\mathbf{f}_n^R = f \mathbf{R} \cdot \mathbf{n}_\xi \quad \text{where } \mathbf{R} = \begin{bmatrix} \cos \kappa d & -\sin \kappa d \\ \sin \kappa d & \cos \kappa d \end{bmatrix} \quad (8)$$

is the orthogonal rotation matrix associated with a rotation of angle  $\kappa d$ . The tangential forces at contact points are then related to their normal counterpart and the friction coefficient  $c$  as follows:

$$\mathbf{f}_t^l = c \mathbf{Q} \cdot \mathbf{f}_n^l = -cf \mathbf{Q} \cdot \mathbf{n}_\xi \quad (9)$$

$$\mathbf{f}_t^R = c \mathbf{Q} \cdot \mathbf{f}_n^R = cf \mathbf{Q} \cdot \mathbf{R} \cdot \mathbf{n}_\xi \quad (10)$$

where  $\mathbf{Q} = [0, -1; 1, 0]$  is the permutation matrix. Finally, the interaction between the dermis and the scale is given by a moment  $m^D$  resisting the rotation of the scale at its attachment point. This is simply written:

$$m^D = K^D (\theta^S - \theta^D) = K^D \theta^S \quad (11)$$

where  $\theta^D$  and  $\theta^S$  are the rotation of the dermis and the scale at their point of intersection and  $K^D$  is the angular stiffness of the attachment. Further, we used the fact that the rotation of the dermis  $\theta^D$  vanishes for the representative scale.

## 2.3. Solution procedure and results

The approach to determine the equilibrium configuration of the representative scale under the various interaction loads is summarized as follows; given a force  $f$ , the equilibrium configuration of the scale deformation and contact forces is found by determining the following three quantities:

- the location  $\xi$  of the point of application of the force  $\mathbf{f}^l$ ,
- the macroscopic curvature  $\kappa$ ,
- the orientation  $\phi(s)$  of the scale centroid.

While the later is found by solving (1),  $\xi$  and  $\kappa$  are found by enforcing the periodicity condition. If we denote the current coordinates of the left and right ends of the primary scale by  $\mathbf{x}_1^p$  and  $\mathbf{x}_2^p$ , respectively, the deformation of scales is periodic if:

$$(\mathbf{x}_2^p - \mathbf{x}_1^p) = \mathbf{R} \cdot (\mathbf{x}_2^R - \mathbf{x}_1^R) \quad (12)$$

where  $\mathbf{x}_1^R$  is the location of the left end of the right scale and  $\mathbf{x}_2^l$  is the coordinates of the right end of the left scale (Fig. 1). The coordinates  $\mathbf{x}_1^p$  and  $\mathbf{x}_1^R$  can be determined from geometrical arguments as:

$$\mathbf{x}_1^p = 0 \quad \text{and} \quad \mathbf{x}_1^R = \frac{1}{\kappa} \begin{bmatrix} \sin \kappa s \\ 1 - \cos \kappa s \end{bmatrix} \quad \text{and} \quad \mathbf{x}_2^l = \mathbf{x}(\xi) \quad (13)$$

Eq. (12) thus leads to a system of two nonlinear equations for  $\kappa$  and  $\xi$ .

$$\mathbf{V}(\xi, \kappa) = \frac{1}{\kappa} \begin{bmatrix} \sin \kappa s \\ 1 - \cos \kappa s \end{bmatrix} + \begin{bmatrix} \cos \kappa d & -\sin \kappa d \\ \sin \kappa d & \cos \kappa d \end{bmatrix} \cdot \mathbf{x}(\xi) - \mathbf{x}_2^p = 0 \quad (14)$$

The procedure then consists of solving (1) and (14) to obtain the unknowns  $(\phi(s), \xi, \kappa)$ . For this, the representative scale is divided in  $(n - 1)$  elements, separated with  $n$  nodes. Following (Vernerey, in preparation), we obtain a finite element equation for the nodal values of the orientation, represented by the  $(n * 1)$  vector  $\Phi$  in the form:

$$\mathbf{U} = \mathbf{K} \cdot (\Phi - \Phi_0) - \mathbf{G} = 0 \quad (15)$$

The final problem to solve is then finding the solution vector  $\mathbf{z} = [\Phi, \xi, \kappa]$  that verifies the system of algebraic equations:

$$\mathbf{R} = \begin{bmatrix} \mathbf{U}(\mathbf{z}) \\ \mathbf{V}(\mathbf{z}) \end{bmatrix} = \mathbf{0} \quad (16)$$

where  $\mathbf{U}$  and  $\mathbf{V}$  are given in (15) and (14), respectively. This equation can be solved with an iterative Newton–Raphson procedure, for which, the solution  $\mathbf{z}^{i+1}$  at the  $(i + 1)$ th iteration is obtained as follows:

$$\mathbf{z}^{i+1} = \mathbf{z}^i - \frac{d\mathbf{R}^i}{d\mathbf{z}} \cdot \mathbf{R}^i \quad (17)$$

The numerical solution is obtained when the norm of the residual  $\mathbf{R}^i$  becomes smaller than a tolerance, defining the accuracy of the solution. Fig. 2 depicts the computed scale deformation for a macroscopic bending of  $\kappa/\ell \approx 1$ , with various values of scale bending and shear stiffness. Generally, if  $t$  is the thickness of the scale, the ratio  $GA/EI$  is comparable to  $1/t^2$ . In other words, a low relative shear resistance will be encountered for thick scales, while a high relative bending stiffness will be encountered when the scales become thin. The figure shows that different scale properties and geometry leads to very different deformation of the fishscale structure. For clarity, the figure depicts the left and right scales, which undergo the same deformation as the primary scale. The results are shown for a scale discrimination of 200 elements. A high number of nodes was necessary in order to accurately capture the location of the contact force.

## 3. Investigation into the mechanics of fishscale structure

In their biological setting, the functions of fishscales are different according to the environment and needs of the fish. The large variety of scale structures found in nature suggest that different functions are attained from quite different architectures. To understand the main trends of this structure/response relationship, the micromechanical model developed in the previous section can be used to quantify how macroscopic bending resistance varies as a function of single scale's size, spacing, properties and interactions.

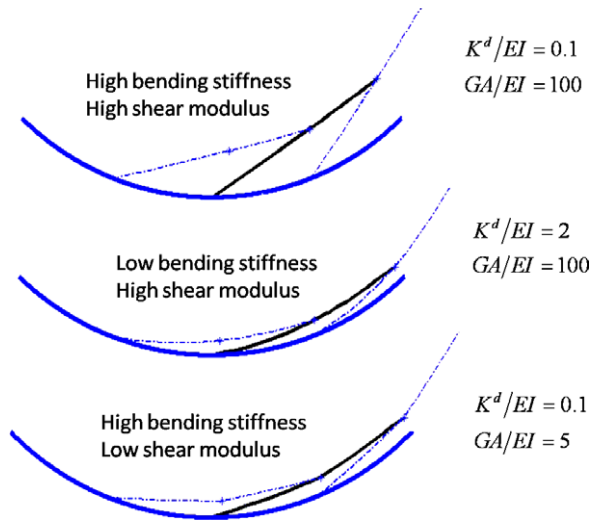


**Fig. 2.** Scale centroid deformation for a macroscopic bending of  $\kappa/\ell \approx 1$ . Three situations are depicted depending on scale properties, relative to the rotational stiffness of the scale-dermis attachment. The  $*$  symbol refers to the contact point  $\mathbf{x}(\xi)$ .

### 3.1. Homogenization procedure

The relation between microscopic forces and macroscopic bending response is obtained by a homogenization procedure, a method that has been documented for a variety of materials and structures (for instance, see Vernerey et al., 2006). In this work, the homogenization procedure aims at relating the forces and moment at the level of a single scale to the macroscopic moment of the entire fishscale structure. Since this macroscopic moment cannot readily be determined from a simple averaging operation, an energetic approach is taken. The approach relies on the fact that the elastic energy stored in the scaled-skin at the macroscale is equal to the cumulative contribution of the stored energy in each single scale of the assembly. Considering a macroscale domain of length  $L$ , for homogeneous bending, the stored elastic energy at the macroscale is written in terms of the macroscopic moment  $M$  and the macroscopic curvature  $\kappa$ :

$$E_{macro} = L \int_{z=0}^{\kappa} M(z) z dz \quad (18)$$

At the microscale, the energy arising from a single scale is written

$$E_{micro} = \int_0^{\ell} \left( \frac{1}{2} E I \kappa_m^2 + \frac{1}{2} A E \epsilon_m^2 + \frac{1}{2} A G \gamma_m^2 \right) ds + \frac{1}{2} K^D (\theta^S)^2 \quad (19)$$

where  $\kappa_m$ ,  $\epsilon_m$  and  $\gamma_m$  are the (microscopic) curvature, axial strain and shear strain in individual scales, respectively and  $K^D$  and  $\theta^S$  were introduced in (11). To relate the two energies, we first note that in a macroscopic length  $L$ , the number of scales is given by  $L/d$ , where  $d$  is the space between scales. The energy equivalence is then written:

$$E_{macro} = \frac{L}{d} E_{micro} \quad (20)$$

Finally, using (18) and (20), the macroscopic moment can be derived by computing the derivative of the microscopic energy with respect to the macroscopic curvature  $\kappa$ :

$$M(\kappa) = \frac{dE_{macro}}{d\kappa} = \frac{L}{d} \frac{dE_{micro}}{d\kappa} \quad (21)$$

where  $E_{micro}$  can be evaluated numerically from (19) for any equilibrium configuration. This leads to a  $(M - \kappa)$  relationship that can be

evaluated for various microscopic parameters (scale properties, size, spacing, etc.).

### 3.2. Effect of scale attachment and scale density

To understand the main mechanisms driving the deformation of scaled-skin, let us first concentrate on a simple system consisting of frictionless scales ( $\mathbf{f}_t = 0$ ), slender scales (no shear deformation) whose bending resistance is given by the product  $EI$  and the attachment resistance by the stiffness  $K^D$ . We thus investigate the effect of two parameters on the macroscale behavior: (i) the ratio  $K^D/EI$  between bending stiffness and attachment stiffness and (ii) the scale density  $\lambda = \ell/d$  defined as the average number of overlapping scales in a cross-section of the skin. Thus,  $\lambda = 1$  is achieved when there is no overlap between scales, and  $\lambda$  increases as scale spacing decreases. Using the definition of scale density, one can also introduce the so-called effective bending stiffness of the structure as  $\lambda EI = E\ell/d$ , which characterizes the bending stiffness of an equivalent homogeneous plate possessing a similar cross-section of the fishscale structure. Finally, as a means to better understand how the micro-deformation affect the macroscopic mechanical response, a measure  $\mathcal{A}$  of the relative contribution of scale rotation and scale deformation can be introduced as:

$$\mathcal{A} = \frac{\theta^S}{\theta^S + \int_0^{\ell} \kappa ds} \quad (22)$$

This parameter provides a convenient measure of the amount of relative scale rotation such as when  $\mathcal{A} = 1$ , macroscopic bending is only due to scale rotation and when  $\mathcal{A} = 0$ , macroscopic bending is only due to bending of individual scales. Fig. 3 shows the results of the parametric study for three values of  $K^D/EI$  (0.1, 1, 10) representing low, moderate and high relative attachment stiffness. For each of these three cases, we considered five values of  $\lambda$  (0.1, 0.3, 0.5, 0.7 and 0.9), ranging from high to low scale overlap. Using standard nondimensionalization, the macroscopic moment  $M$  is normalized by the effective bending stiffness  $E\ell/d$  and the macroscopic curvature  $\kappa$  is normalized by the scale length  $\ell$ . Finally, the deformed configuration of individual scales and the associated value of  $\mathcal{A}$  are plotted to better understand the correlation between macro- and micro- responses. The below results highlight a few important features of fishscale structure mechanics.

- For given scale stiffness  $EI$ , the normalized bending stiffness  $K_B$  of the structure increases in a nonlinear fashion with the attachment stiffness  $K^d$  and increases linearly with scale density. The relationship between  $K_B$  and normalized attachment stiffness  $K^D/EI$  is shown in Fig. 4.
- As scale attachment stiffens and scale fraction increases, the macroscopic response converges to that of a homogeneous plate of stiffness  $\frac{E\ell}{d}$ .
- Strain-stiffening is an inherent characteristic of the mechanical response of fishscale in bending. This stiffening is especially pronounced when  $\mathcal{A}$  is small (due to the large scale rotation associated with weak attachment stiffness  $K^D/EI$ ) and disappears when  $\mathcal{A}$  is close to unity (associated with large attachment stiffness  $K^D/EI$ ).
- Contact force (normalized by the macroscopic moment) between scales increases significantly with scale density and appears to be independent of the ratio  $K^D/EI$ . This trend is given in Fig. 4.

### 3.3. Effect of shear and interscale friction

Typically, increasing a scale's resistance to bending involves increasing its moment of inertia, or in other terms, its thickness

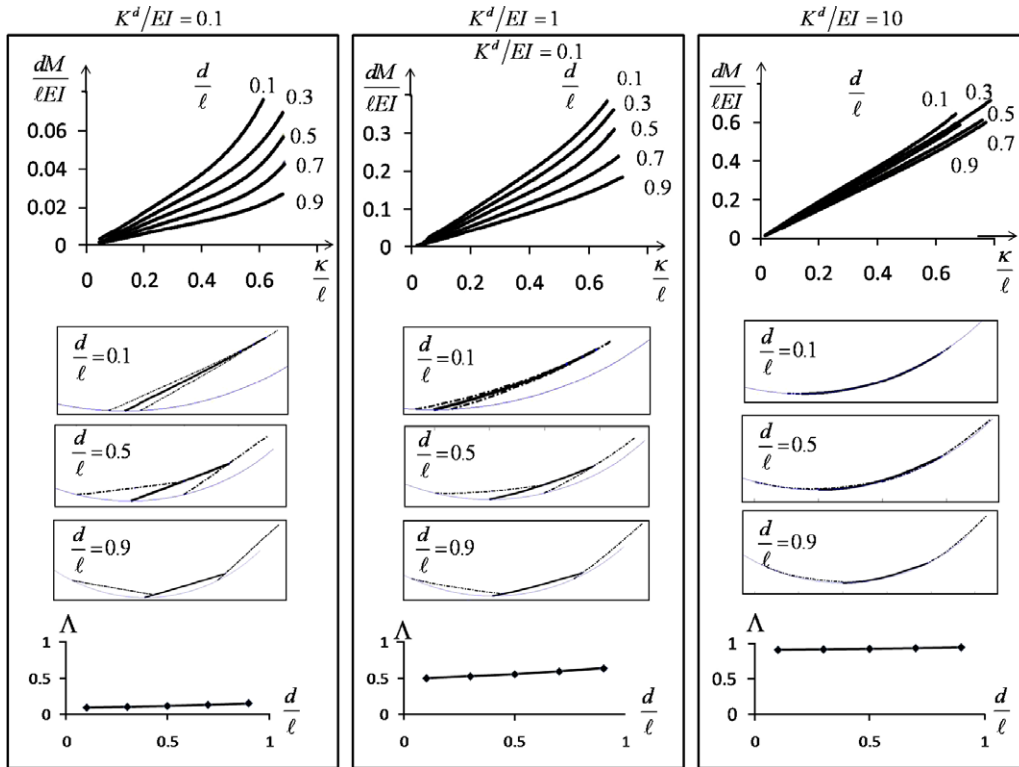


Fig. 3. Effect of scale attachment and scale overlap on the macroscopic behavior of fishscale structure.

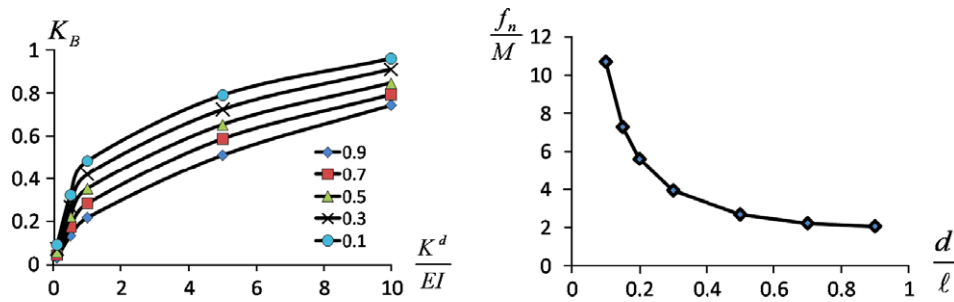


Fig. 4. Variation of stiffness and contact force with scale fraction.

(since one considers scales as homogeneous plates in this study). However, as thickness becomes larger, the effects of shear deformation are known to become increasingly important. Fig. 5 shows the effect of the shear resistance  $GA/EI$  (relative to bending resistance) on the macroscopic bending moment response. While the figure concentrates on the case where  $d/l = 0.5$  and  $K^D/EI = 1$ , similar trends can be shown for other cases; both average stiffness and

strain-stiffening decrease with the shear modulus. Observing the structure's deformation (Fig. 5, right) indicates that for lower shear stiffness, a localized shear deformation appears at the contact point between scales. As a consequence, large scale deformation occurs with a very small stored elastic energy, which explains the decreasing stiffness with decreasing shear stiffness  $GA$ . Finally, the role of inter-scale friction was assessed. For the range of

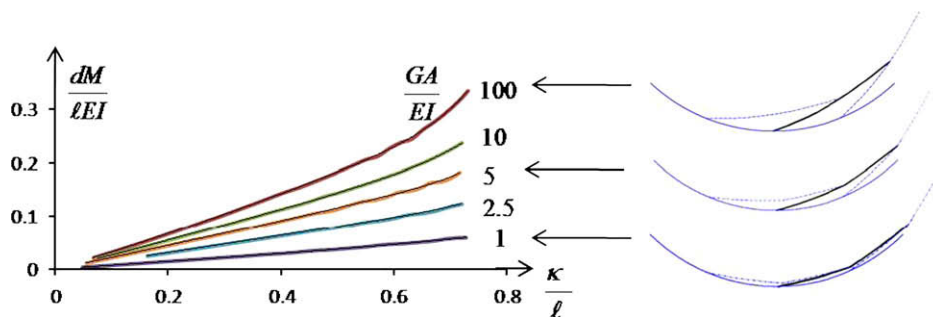


Fig. 5. Effect of scale relative shear resistance  $GA/EI$  on the macroscopic response of fishscale structures.

curvature being investigated ( $\kappa/\ell < 1$ ), we found that the role of friction on the overall bending stiffness is negligible. This trend was true for all scale fraction and ratio  $K^D/EI$  investigated in this paper.

#### 4. Discussion

An important result of this study is the presence of a strain-stiffening mechanism in fishscale structure. Strain-stiffening response is a characteristic shared by a large number of biological structure and materials (Storm et al., 2007) as a way to prevent structural damage and failure. Indeed, a strain-stiffening material will tend to redistribute deformation over a large region in order to minimize the stored elastic energy. This feature ensures that stresses are dispersed throughout the structure. The present study showed that the strain-stiffening mechanism is highly dependent on the ratio between scale attachment stiffness and scale bending stiffness. It is also significantly affected by the scale density. In short, the more pronounced strain-stiffening was found for a very small values of  $K^D/EI$  and for large scale densities. On the other side of the spectrum, for large values of the scale attachment stiffness, the behavior of the fishscale structure was converging to the response of a homogeneous plate, displaying no strain-stiffening.

This feature plays may play a significant role in protecting fish predator attack in the form of biting. From a mechanical view point, this situation can be compared to the indentation of a soft material (the fish body) covered with fishscales. As shown in the bottom figure of Fig. 6, the fishscale structure will (i) redistribute the curvature in a region whose size is proportional to scale size and (ii) due to the strain-stiffening response, an increasing indenting force will result in an increase of strain redistribution until failure of the indented scale occurs.

Both features will contribute in minimizing force concentration, redistributing energy within the structure and thus postponing final failure. In addition, the role of fishscale as an external tendon is plausible, since the stored energy, which increases with curvature, may be restituted to the fish to increase locomotion speed. The scale-structure could then be compared to a bouncing spring, converting its stored elastic energy into kinetic energy. While these results seem to indicate that the overall properties fish-structure display the highest strain-stiffening for a very small attachment stiffness and high scale density, criteria other than strain stiffening must also be considered. In Fig. 4a, the average macroscopic bending stiffness (in the range  $0 < \frac{\kappa}{\ell} < 1$ ) is shown in terms of the ratio  $K^D/EI$ . These curves clearly show that this stiffness converges to zero as  $K^D$  becomes smaller. This situation is not acceptable as a very small stiffness would provide no structural protection to fish. The nonlinear relation between micro and macro stiffness indicates that there should be an optimum value of the ratio  $K^D/EI$  such

that the best combination of stiffness and strain-stiffening is achieved. Normal contacting force between adjacent scale is also an important factor to consider, as it is the cause of potential scales failure. Fig. 4 shows that increasing scale density has the effect of magnifying the magnitude of this force. In other words, a high scale density is not desirable as it would favor an early fracture of individual scales.

#### 5. Conclusion

In this study, we investigated the bending response of fishscale structure in terms of its local geometry and properties. We showed that for certain microscale features, the response exhibits a strain-stiffening response, which can play a large role in preventing local unstable deformation that can threaten a fish during swimming and predator attack. Generally our results indicate that:

- Strain-stiffening characteristic increases with increasing scale density and decreasing scale-dermis attachment rotational stiffness (relative to a scale's bending stiffness).
- The contact force (relative to macroscopic moment) between scales increases exponentially with a measure of scale density.
- The average macroscopic bending stiffness increases in a non-linear fashion with the ratio  $K^D/EI$ .
- Finally, shear deformation of the scale tends to decrease both the average stiffness and the strain-stiffening characteristic of the fishscale response.

Fig. 7 summarizes these trends. According to its environment and size, a species of fish may emphasize certain functions over others. For instance, in cases where locomotion speed is emphasized, the structure will be “designed” in terms of the strain-stiffening (role of external tendon) and light-weight. On the other hand, if protection against predator is critical, the design will favor a higher resistance to fracture and average bending stiffness. This flexibility in choice may explain the large diversity of scale structures encountered in nature, from large to small scale, high to low density, all of them within region of acceptable design depicted by the grey region in Fig. 7. The presented thus present an attractive framework with which one can better understand the function of a fishscales in different fish species. Indeed, if one can quantify a fishscale structure by few parameters (as depicted in Table 1 for the striped bass), it possible to predict its underlying mechanics (bending response, internal stress concentration, etc.) and gain fundamental information with regards to its potential functions.

It is also important to realize that the presented model is highly idealized and can only be used to assess general trends in the mechanics of fishscale structures. In particular, the model's

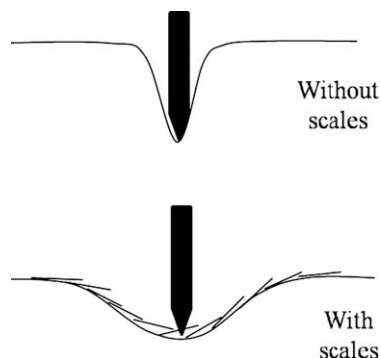


Fig. 6. Illustration of the role of fishscales in preventing unstable localized deformation.

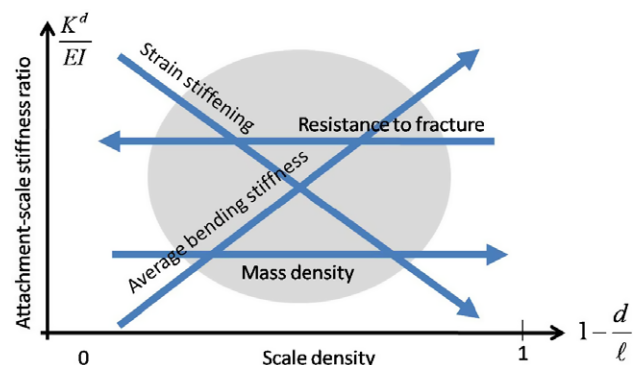


Fig. 7. Trends in fishscale response in terms of its underlying microstructure.

**Table 1**  
Typical parameters for natural fishscale structures.

Parameter	Value	Source
Scale thickness	0.1 mm	Measured on stripped bass ( <i>Morone saxatilis</i> )
Scale diameter	10 mm	Measured on stripped bass ( <i>Morone saxatilis</i> )
Scale overlap	5 mm	Measured on stripped bass ( <i>Morone saxatilis</i> )
Young's modulus	2.2 GPa	Ikoma et al. (2003)
Poisson's ratio	0.4	Typical for polymers
Friction coefficient	0.04–0.6 range	Typical for polymer friction (ref below)
Angular stiffness $K_d$	No available data	

limitations can be overcome by considering the following aspects into future research:

- As mentioned earlier, the incorporation of the underlying skin elasticity and its effect on the effective properties can be of interest in certain conditions (Brainerd, 1994a,b). The proposed methodology can be extended by considering the “scale and skin” system instead of the “scale” system.
- Real fishscale structures are three-dimensional in nature. In comparison to a two-dimensional structure such as studied in this paper, the different possibilities for structural parameters (such as scale shape and arrangement) are endless. In terms of mechanical behavior, multidimensional elasticity will display a richer variety of response, including in plane scale deformations and anisotropy. In spite of those differences, the methodology introduced in this paper can be extended in three-dimension and is the object of current research in our group.
- Finally, in order to understand how fishscales participate into the mechanics of fish-swimming and fish biomechanics, it will be essential to couple model of fishscale with other organs, including skeleton, muscle and tendons (Shadwick and Lauder, 2006).

Finally, besides advancing our knowledge into the mechanics of biological materials and structure, this work will provide a fundamental basis into the bio-inspired design of thin, protective structures (such as body armors, exoskeletons or protection for morphing flexible structures).

### Acknowledgment

The authors wish to acknowledge the support of the National Science Foundation under award CMMI 0927585.

### Appendix A

In Eq. (2), the matrix  $\mathbf{P}_1$  is given by:

$$\mathbf{P}_1 = \begin{bmatrix} -\sin 2\phi & \cos 2\phi \\ \cos 2\phi & \sin 2\phi \end{bmatrix} \quad (23)$$

and the vector  $\mathbf{w}$  and matrix  $\mathbf{P}_2$ , introduced in (6) have the form:

$$\mathbf{w} = \begin{pmatrix} \cos \phi \\ \sin \phi \end{pmatrix} \quad \text{and} \quad \mathbf{P}_2 = \begin{bmatrix} \beta + \alpha \cos 2\phi & \alpha \sin 2\phi \\ \alpha \sin 2\phi & \beta - \alpha \cos 2\phi \end{bmatrix} \quad (24)$$

where

$$\beta = \frac{1}{2} \left( \frac{1}{EA} + \frac{1}{kGA} \right) \quad (25)$$

The force integral function  $\mathbf{F}$  is generally defined as:

$$\mathbf{F} = \int_0^L \mathbf{f}(s) ds \quad (26)$$

where  $\mathbf{f}$  are the forces acting on the scale (beam) centroid. For the representative scale studied in this paper, it is straightforward to show that the function  $\mathbf{F}$  becomes:

$$\mathbf{F}(s, \phi_1, \kappa) = \{h(s)\mathbf{R}(\phi(\xi)) - \mathbf{R}(\phi(\xi) + \kappa d)\} \cdot \mathbf{f} \quad (27)$$

where  $h$  is the step function defined by

$$h(s) = \begin{cases} 1 & \text{if } s < s_1 \\ 0 & \text{if } s > s_1 \end{cases} \quad \text{and} \quad \mathbf{f} = \begin{bmatrix} 0 \\ f \end{bmatrix} \quad (28)$$

### References

- Ballarini, R., Kayacan, R., Ulm, F.J., Belytschko, T., Heuer, A.H., 2005. Biological structures mitigate catastrophic fracture through various strategies. *International Journal of Fracture* 135 (1–4), 187–197.
- Barthelat, F., 2007. Biomimetics for the next generation materials. *Philosophical Transactions of the Royal Society A – Mathematical Physical and Engineering Sciences* 365, 2907.
- Barthelat, F., Tang, H., Zavattieri, P.D., Li, C.M., Espinosa, H.D., 2007. On the mechanics of mother-of-pearl: a key feature in the material hierarchical structure. *Journal of the Mechanics and Physics of Solids* 55 (2), 225–444.
- Brainerd, E.L., 1994a. Mechanical design of polypterid fish integument for energy storage during recoil aspiration. *Journal of Zoology* 232, 7–19.
- Brainerd, E.L., 1994b. Pufferfish inflation: functional morphology of postcranial structures in *Diodon holocanthus* (tetraodontiformes). *Journal of Morphology* 220, 243–261.
- Bruet, B., Song, J., Boyce, M., Ortiz, C., 2008. Materials design principles of ancient fish armour. *Nature Materials* 7, 748–756.
- Chen, L., Ballarini, R., Kahn, H., Heuer, A.H., 2007. Bioinspired micro-composite structure. *Journal of Materials Research* 22 (1), 124–131.
- Fratzl, P., Weinkamer, R., 2007. Nature's hierarchical materials. *Progress in Materials Science* 52 (8), 1263–1334.
- Gibson, L.J., Ashby, M.F., Karam, G.N., Wegst, U., Shercliff, H.R., 1995. The mechanical-properties of natural materials. 2. Microstructures for mechanical efficiency. *Proceedings of the Royal Society of London Series A – Mathematical and Physical Sciences* 450 (1938), 141–162.
- Hebrank, M.R., 1982. Mechanical-properties of fish backbones in lateral bending and in tension. *Journal of Biomechanics* 15 (2), 85–89.
- Hebrank, M.R., Hebrank, J.H., 1986. The mechanics of fish skin – lack of an external tendon role in 2 teleosts. *Biological Bulletin* 171 (1), 236–247.
- Ikoma, T., Kobayashi, H., Tanaka, J., Walsh, D., Mann, S., 2003. Physical properties of type I collagen extracted from fish scales of *Pagrus major* and *Oreochromis niloticus*. *International Journal of Biological Macromolecules* 32 (3–5), 199–204.
- Kardong, K., 2008. *Vertebrates: Comparative Anatomy, Function, Evolution*, second ed. McGraw-Hill.
- Long, J.H., Hale, M.E., McHenry, M.J., Westneat, M.W., 1996. Functions of fish skin: flexural stiffness and steady swimming of Longnose gar *Lepisosteus osseus*. *Journal of Experimental Biology* 199 (10), 2139–2151.
- Long, J.H., Adcock, B., Root, R.G., 2002. Force transmission via axial tendons in undulating fish: a dynamic analysis. *Comparative Biochemistry and Physiology A – Molecular and Integrative Physiology* 133 (4), 911–929.
- Long, J.H., Koob, T.J., Irving, K., Combie, K., Engel, V., Livingston, N., Lammert, A., Schumacher, J., 2006. Biomimetic evolutionary analysis: testing the adaptive value of vertebrate tail stiffness in autonomous swimming robots. *Journal of Experimental Biology* 209 (23), 4732–4746.
- Meyers, M.A., Lin, A.Y.M., Seki, Y., Chen, P.Y., Kad, B.K., Bodde, S., 2006. Structural biological composites: an overview. *JOM* 58 (7), 35–41.
- Sanchez, C., Arribart, H., Guille, M.M.G., 2005. Biomimeticism and bioinspiration as tools for the design of innovative materials and systems. *Nature Materials* 4 (4), 277–288.
- Shadwick, Lauder, 2006. *Fish Biomechanics*. Elsevier. vol. 23.
- Storm, C., Pastore, J., McKintosh, J., Lubensky, T., Janmey, P., 2007. Nonlinear elasticity in biological gels. *Nature* 435, 191–194.
- Sudo, S., Tsuyuki, K., Ito, Y., Ikohagi, T., 2002. A study on the surface shape of fish scales. *JSM International Journal Series C – Mechanical Systems Machine Elements and Manufacturing* 45 (4), 1100–1105.
- Tang, Z., Kotov, N., Magonov, S., Ozturk, B., 2003. Nanostructured artificial nacre. *Nature Materials* 2, 413–418.
- Vernerey, F.J., McVeigh, C., Liu, W.K., Moran, B., Tewari, D., Parks, D., Olson, G., 2006. The 3-d computational modeling of shear-dominated ductile failure in steel. *The Journal of The Minerals Metals and Materials Society*, 433–445.
- Vernerey, F.J., K Liu, W., Moran, B., 2007a. Multi-scale micromorphic theory for hierarchical materials. *Journal of the Mechanics and Physics of Solids* 55, 2603–2651.
- Vernerey, F.J., Liu, W.K., Moran, B., Olson, G., 2007b. A micromorphic model for the multiple scale failure of heterogeneous materials. *Journal of the Mechanics and Physics of Solids* 56, 1320–1347.
- Vernerey, F.J., Liu, W.K., Moran, B., Olson, G., 2009. Multi-length scale micromorphic process zone model. *Computational Mechanics* 44, 45–51.
- Vernerey, F.J., in preparation. On a reduced beam formulation with kinematic constraints and its application to multi-fiber systems. *Computers and Structures*.
- Vincent, J.F.V., Bogatyrev, O.A., Bogatyrev, N.R., Bowyer, A., Pahl, A.K., 2006. Biomimetics: its practice and theory. *Journal of the Royal Society Interface* 3 (9), 471–482.